Article

Cell Reports

Oscillatory Dynamics in the Frontoparietal Attention Network during Sustained Attention in the Ferret

Graphical Abstract

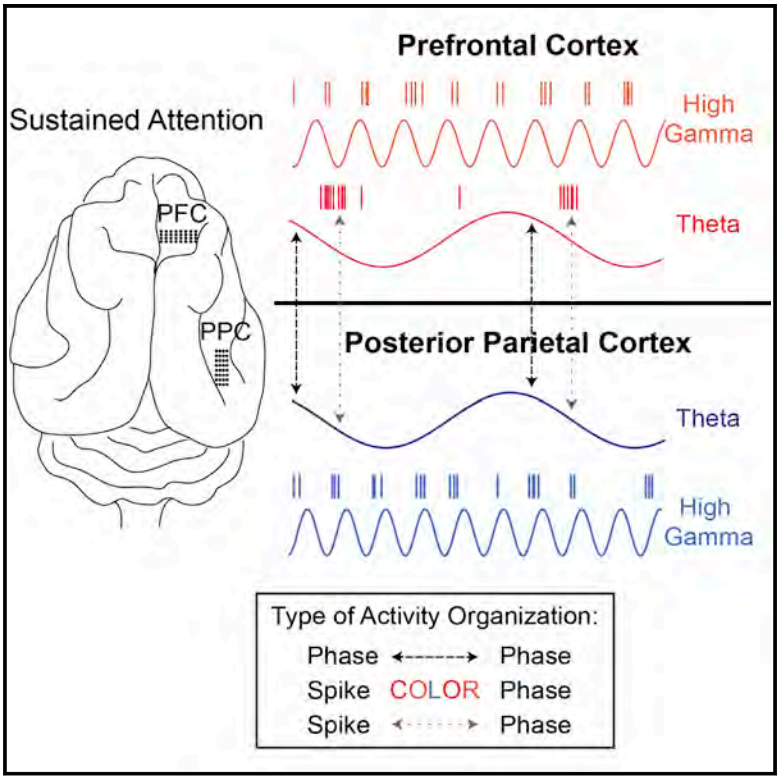

Highlights

- PFC and PPC exhibit task-dependent theta synchronization during sustained attention
- Frequency-specific local and long-range activity during sustained attention
- Spiking in PFC phase locks to local and long-range theta oscillations
- Both PFC and PPC single units phase lock to local high gamma activity

Authors

Kristin K. Sellers, Chunxiu Yu, Zhe Charles Zhou, ..., Susanne Radtke-Schuller, Sankaraleengam Alagapan, Flavio Fröhlich

Correspondence

flavio_frohlich@med.unc.edu

In Brief

Sellers et al. investigate the neural correlates of sustained attention in the frontoparietal network using electrophysiology in the prefrontal and posterior parietal cortices. They demonstrate that theta oscillations mediate synchronization of PFC and PPC in a task-dependent manner. Spiking activity was coordinated by local and long-range activity, relying on different frequencies.

Sellers et al., 2016, Cell Reports *16*, 2864–2874
September 13, 2016
http://dx.doi.org/10.1016/j.celrep.2016.08.055

OPEN ACCESS
CellPress

Cell Reports
Article

Oscillatory Dynamics in the Frontoparietal Attention Network during Sustained Attention in the Ferret

Kristin K. Sellers,[1,2] Chunxiu Yu,[1] Zhe Charles Zhou,[1,2] Iain Stitt,[1] Yuhui Li,[1] Susanne Radtke-Schuller,[1] Sankaraleengam Alagapan,[1] and Flavio Fröhlich[1,2,3,4,5,6,7,*]
[1]Department of Psychiatry
[2]Neurobiology Curriculum
[3]Department of Cell Biology and Physiology
[4]Department of Biomedical Engineering
[5]Neuroscience Center
[6]Department of Neurology
University of North Carolina at Chapel Hill, Chapel Hill, NC 27599, USA
[7]Lead Contact
*Correspondence: flavio_frohlich@med.unc.edu
http://dx.doi.org/10.1016/j.celrep.2016.08.055

SUMMARY

Sustained attention requires the coordination of neural activity across multiple cortical areas in the frontoparietal network, in particular the prefrontal cortex (PFC) and posterior parietal cortex (PPC). Previous work has demonstrated that activity in these brain regions is coordinated by neuronal oscillations of the local field potential (LFP). However, the underlying coordination of activity in terms of organization of single unit (SU) spiking activity has remained poorly understood, particularly in the freely moving animal. We found that long-range functional connectivity between anatomically connected PFC and PPC was mediated by oscillations in the theta frequency band. SU activity in PFC was phase locked to theta oscillations in PPC, and spiking activity in PFC and PPC was locked to local high-gamma activity. Together, our results support a model in which frequency-specific synchronization mediates functional connectivity between and within PFC and PPC of the frontoparietal attention network in the freely moving animal.

INTRODUCTION

State- and behavior-dependent modulation of cortical oscillations is ubiquitous in both humans and animal models (Buzsáki and Draguhn, 2004; Engel et al., 2001). The hierarchical organization of oscillatory activity is particularly important for inter-area organization (Lisman and Jensen, 2013). The synchronization of oscillations across brain regions has been suggested to underlie effective communication across neuronal groups (Fries, 2005; Sarnthein et al., 1998; Varela et al., 2001). Within neuronal ensembles, synchronization in the gamma frequency band is commonly found in activated networks and increases the strength of neuronal input to other regions (Fries, 2009). Oscillatory activity appears to coordinate neuronal spiking within and across multiple brain regions (Canolty et al., 2010). Such preferential spiking activity, organized according to the phase of frequency-specific oscillations, is particularly important for the encoding of discrete information, such as different objects in memory (Siegel et al., 2009). When oscillatory coupling becomes pathologically strong or weak, local spike synchrony becomes perturbed and neuronal communication is disrupted (Voytek and Knight, 2015). However, we still do not have a clear understanding of the multiplexed organization of spiking and oscillatory activity within and across brain regions.

Visual attention is ideal for investigating the organization of intra- and inter-area interaction dynamics since it requires coordination of activity both within and across brain regions (Clayton et al., 2015; Posner and Petersen, 1990; Womelsdorf and Fries, 2007), potentially with frequency-specific structure. Here, we focus on sustained attention, which can be defined as the selective prioritization of the neural representations of a specific task for a continuous amount of time (Buschman and Kastner, 2015). The activation of a number of cortical (frontal, parietal, temporal, and occipital) as well as subcortical (thalamic and midbrain) regions is commonly observed in attention task-related fMRI studies (Petersen and Posner, 2012; Scolari et al., 2015; Langner and Eickhoff, 2013; Corbetta and Shulman, 2002). In particular, the frontoparietal attention network is activated during attention-demanding visuospatial tasks (Katsuki and Constantinidis, 2012). Limited work has shown that prefrontal cortex (PFC) and posterior parietal cortex (PPC) exhibit LFP synchrony in beta (22–34 Hz) and gamma (35–55 Hz) frequencies in the head-fixed non-human primate during top-down and bottom-up attention, respectively (Buschman and Miller, 2007). However, the neurophysiological correlates of sustained attention at the finer-timescale of organizing single unit (SU) activity are less clear. Furthermore, little is known about the interaction dynamics of these areas during naturalistic freely moving behavior,

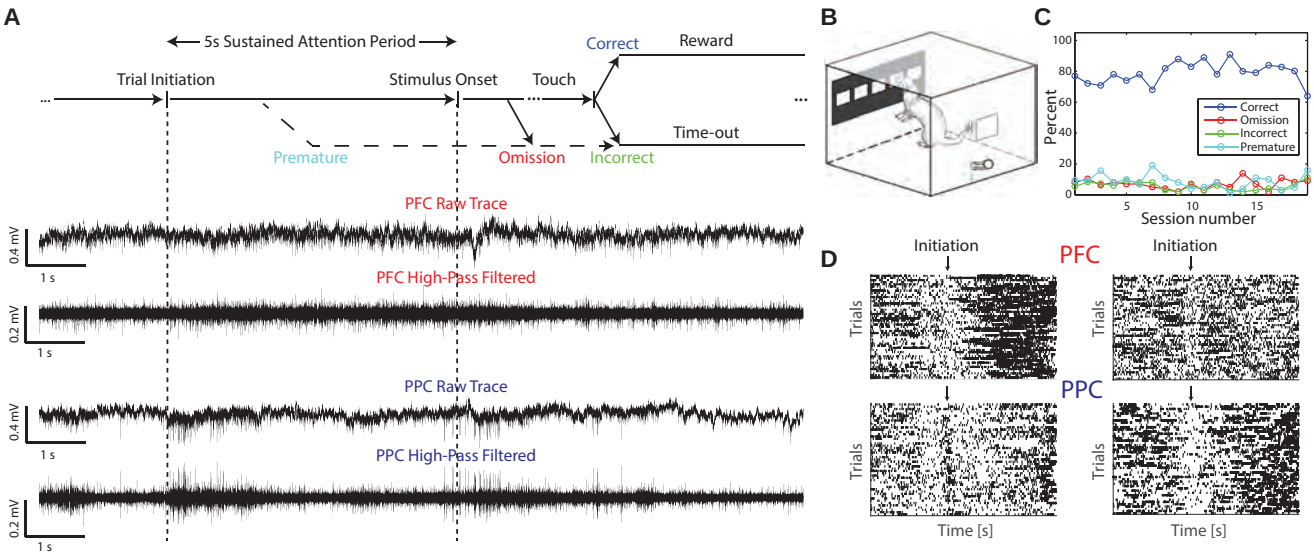

Figure 1. Animals Performed a Sustained Visual Attention Task during Simultaneous Electrophysiological Recordings in Prefrontal Cortex and Posterior Parietal Cortex

(A) Top: the 5-CSRTT was a self-paced task. The animal initiated each trial at the lick spout starting a 5-s sustained attention period, after which a stimulus appeared in one of five windows. Correct responses resulted in delivery of a water reward. Bottom: The electrophysiological signals were continuously recorded to provide LFP and spiking activity information.

(B) Behavioral chamber with five response windows on a touch screen at one end and a lick spout at the other end.

(C) After training, animals performed at approximately 80% of trials correct per session. Behavioral performance for Animal C is shown, see Figure S1 for other animals.

(D) Raster plots of two SUs each in PFC and PPC aligned to trial initiation show task modulation in firing rate. The units showed heterogeneous changes in firing rate across time.

given that traditional head-fixed paradigms preclude natural movement and impose an artificial state of limited behavior. To fill this gap, we investigated LFP oscillations and SU activity and their relationship both within and between PFC and PPC in the freely moving ferret during a task that requires visual sustained attention, the 5-choice serial reaction time task (5-CSRTT) (Carli et al., 1983; Bari et al., 2008). There is growing evidence that the synchronized neuronal activity underlying low-frequency oscillations mediates long-range organization, while neuronal activity contributing to higher-frequency gamma oscillations organizes local activity (von Stein et al., 2000; Kopell et al., 2000). It has not been fully elucidated if the same frequency structure applies to the fine temporal scale of spiking activity organization across brain areas. Thus, as an extension of the aforementioned electroencephalogram (EEG) and modeling findings, we hypothesized that local organization of spiking activity during sustained attention is mediated by high-frequency activity, whereas long-range organization relies on low-frequency oscillations.

RESULTS

Animals performed a sustained attention task, the 5-CSRTT, during simultaneous recording of LFP and spiking activity in PFC and PPC (Figures 1A, 1B, and 1D). In this self-paced task, animals initiated trials to start a 5 s sustained attention period, during which no stimuli were presented. Correct response of the animal touching the window where the stimulus was presented resulted in a water reward. Animals performed this task with high accuracy (Figure 1C, performance of Animal C; see Figure S1 for performance of other animals; mean percent correct trials across recording sessions ± SD: Animal A = 81.8 ± 7.89; Animal B = 78.2 ± 9.39; and Animal C = 78.9 ± 7.01). We focused on the time period 5 s prior to trial initiation to 7 s after initiation, which encompassed the 5 s sustained attention period of interest. Subsequent analyses included only trials with correct behavioral responses in which the animal was facing the screen at the time of stimulus onset. For a subset of analyses, we also looked at neuronal activity aligned to correct touch. In total, we analyzed 42 sessions (Animal A = 7, Animal B = 16, and Animal C = 19) with a total of 2,418 trials (mean number of correct trials per recording ± SD: Animal A = 35.14 ± 7.47; Animal B = 50.88 ± 22.27; and Animal C = 71.47 ± 9.06). Signals recorded on electrode arrays were spike sorted, and we analyzed 458 SUs in PFC (Animal A = 155, Animal B = 172, and Animal C = 131) and 397 SUs in PPC (Animal A = 193, Animal B = 142, and Animal C = 62).

The frontoparietal attention network in humans and monkeys exhibits rich anatomical connectivity (Szczepanski et al., 2013; Cavada and Goldman-Rakic, 1989). Since nothing is known about the frontoparietal attention network in the ferret, we conducted a separate tracing study (n = 4 animals) to determine if PFC and PPC exhibit direct anatomical connectivity. We performed anterograde tracing using rAAV5-CaMKII-GFP injected into PFC (Figures 2A–2C and S2A–S2C) and retrograde tracing using cholera toxin subunit B (CTB) injected into PPC (Figures 2D–2F and S2D–S2F). Results from both of these tracing

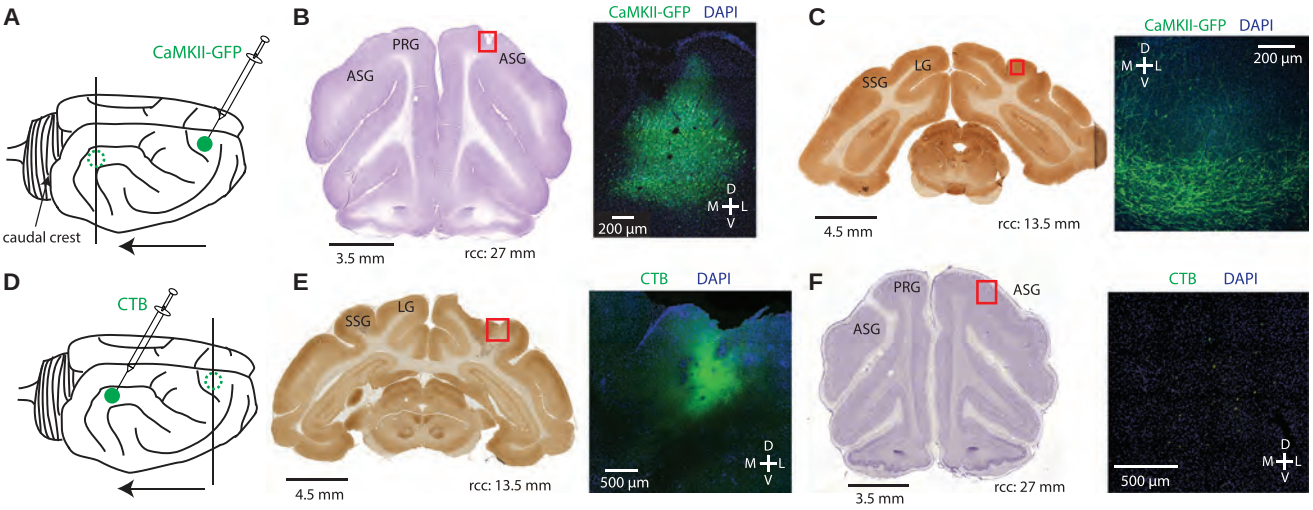

Figure 2. Anterograde and Retrograde Tracing Demonstrate Anatomical Connectivity between PFC and PPC

See Figure S2 for additional animals.

(A) rAAV5-CamKII-GFP was injected in PFC for anterograde tracing (solid circle). The expression was assessed in PPC (dashed circle). The arrow indicates the direction of the anatomical connections elucidated.

(B) GFP was injected in PFC at 27 mm relative to caudal crest (rcc). The red square in the neighboring section stained for Nissl indicates the location of the fluorescent image on the right. The injection site in PFC shows robust labeling of cell bodies; green = GFP, blue = DAPI counterstain, ASG = anterior sigmoid gyrus, PRG = proreal gyrus.

(C) Cytochrome oxidase stained neighboring section in PPC (13.5 mm rcc). The red square indicates the location of the fluorescent image on the right. The projections in PPC exhibit GFP labeling, indicating direct anatomical connections from the injection site location; SSG = suprasylvian gyrus, LG = lateral gyrus.

(D) CTB-488 was injected in PPC for retrograde tracing (solid circle). The expression was assessed in PFC (dashed circle). The arrow indicates the direction of the anatomical connections elucidated.

(E) CTB-488 was injected into PPC. The red square in the neighboring section stained for cytochrome oxidase indicates the location of the fluorescent image on the right.

(F) PFC exhibits expression of CTB-488. The red square in the section stained for Nissl indicates the location of the fluorescent image on the right.

methods were in agreement and demonstrated direct anatomical connections from PFC to PPC. Recording locations were verified with histology (Figure S3) and correspond to the PFC and PPC locations from the tracing study.

Task-Modulated Spiking Activity and Spectral Power in Select Frequencies

We first investigated how spiking activity was modulated during the task (Figure 3). We found 86.7% of PFC units and 85.1% of PPC units were modulated during the peristimulus period (−5 to 7 s relative to initiation) (Figure 3A left, percent of significantly task-modulated PFC units for each animal shown in color: Animal A = 80.7%, Animal B = 89.5%, and Animal C = 90.1%; Figure 3B left, PPC units: Animal A = 77.2%, Animal B = 94.4%, and Animal C = 88.7%). The largest breakpoints for each significantly modulated unit indicate at what time the greatest change in firing rate occurred (Figures 3A and 3B, right).

Next, we looked for modulation of LFP spectral power during the task, defined as an increase or decrease of spectral power. The PFC spectra reflected 1/f properties with no local maxima (Figure 3C, left, averaged across recording sessions for Animal C). Delta, theta, and alpha power were significantly lower following touch compared to both before and after initiation (ANOVA, delta: $F(2, 7{,}392) = 174$, $p < 0.001$; theta: $F(2, 7{,}392) = 182.1$, $p < 0.001$; and alpha:$(F(2, 7{,}392) = 19.6$, $p < 0.001$). However, power was not different before and after initiation for any frequency band. There were no differences between before initiation, after initiation, and after touch in beta power ($F(2, 7{,}392) = 0.12$, $p = 0.89$) or gamma power ($F(2, 7{,}392) = 0.6$, $p = 0.55$). Overall, all these differences were quite small.

In contrast, PPC exhibited a local peak in activity at 5 Hz (theta) (Figure 3C, right, averaged across recording sessions for Animal C, insets show example traces of LFP activity in the theta frequency band after initiation and after touch). Delta and theta power were both task modulated (ANOVA, delta: $F(2, 7{,}392) = 97.5$, $p < 0.001$ and theta: $F(2, 7{,}392) = 309.4$, $p < 0.001$). Delta and theta power were strongest after initiation, showing a 1.23% and 1.5% increase compared to before initiation and after touch, respectively. Alpha and beta power were stronger after touch compared to before and after initiation (alpha: $F(2, 7{,}392) = 167.1$, $p < 0.001$ and beta: $F(2, 7{,}392) = 253.4$, $p < 0.001$), and there was no significant difference between before and after initiation. Gamma and high gamma (80–120 Hz) power were modestly increased during the sustained attention period compared to baseline (0.7% and 0.6% increase, respectively), but there was no difference between after touch and either condition ($F(2, 7{,}392) = 6.56$, $p = 0.001$). Overall, changes in spectral power were very small during the task. Because of the spectral peak in theta and our original hypothesis, we chose to focus our subsequent investigation on the organization of local and long-range activity within the theta, gamma, and high gamma frequency bands.

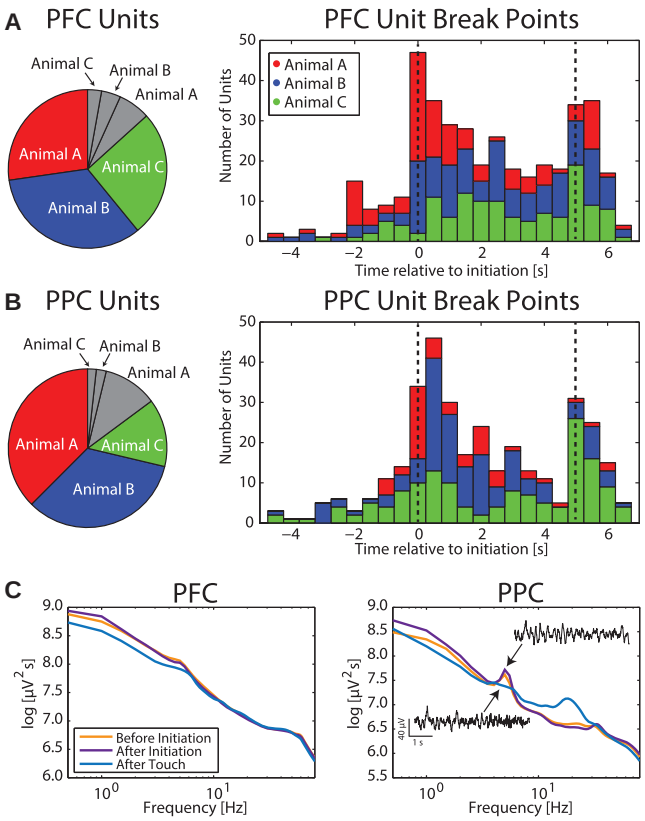

Figure 3. Task-Dependent Modulation of Single Unit Spiking and Spectral Activity

(A) Left: 86.7% of PFC units across all animals showed significant modulation during the peristimulus period (−5 to 7 s relative to trial initiation). The colored pie pieces indicate significantly modulated units for each animal, while the gray pieces show units with non-significant modulation. Right: The distribution of the largest break point for each significantly modulated PFC unit is shown. Structural change in spiking activity was most prominent during the sustained attention period. The dashed lines indicate trial initiation and stimulus onset times.

(B) Left: 85.1% of PPC units across all animals exhibited significant modulation during the peristimulus period. The colors are as in (A). Right: In PPC, the distribution of the largest break point for each significantly modulated unit is shown. Structural change in spiking activity was most prominent immediately following trial initiation and at stimulus onset.

(C) Spectra show average power before initiation (−5 to 0 s relative to initiation), after initiation (0 to 5 s relative to initiation), and after touch (0 to 5 s relative to touch). Left: PFC exhibited 1/f structure with little spectral modulation. Right: In PPC, a prominent 5 Hz peak was evident before and after trial initiation, but not following touch. The insets show example LFP activity filtered in the theta frequency band.

Effective Connectivity and Task-Modulated Theta Phase Synchronization between PFC and PPC

Having demonstrated that select LFP frequencies exhibit task-dependent modulation in power, we next asked if activity in PFC and PPC was coordinated within these frequency bands. To assess synchronization between these areas across time and frequency, we calculated the phase-locking value (PLV) (Lachaux et al., 1999) between simultaneously recorded channel pairs in PFC and PPC (mean number of electrode pairs for each recording ± SD: Animal A = 779.14 ± 131.76, Animal B = 683.53 ± 212.55, and Animal C = 498.32 ± 221.31). PLV can be conceptualized as a metric assessing connectivity or phase synchronization between two brain regions. We found prominent 5 Hz theta phase synchronization before trial initiation (−3 to −1 s relative to trial initiation) and after trial initiation (1 to 3 s relative to initiation), but absence of phase synchronization following correct touch response (1 to 3 s relative to touch). A momentary disruption in this between-area communication was also evident at the time of trial initiation (−0.5 to 0.5 s relative to trial initiation) (Figure 4A, phase at 5 Hz of example raw traces from a single channel pair; Figure 4C, significant PLV for Animal A across recordings; and Figure S4). For all animals, 5 Hz was the most prominent carrier frequency of between-region phase synchronization (Figure 4B). The periods before initiation and after initiation showed the most prominent phase locking and were not significantly different in strength (paired t test, before initiation versus after initiation: $t(41) = -0.29$, $p = 0.77$). Strikingly, phase locking between PFC and PPC was abolished after touch (Figure 4D, paired t test, before initiation versus after touch: $t(41) = 9.25$, $p < 0.001$ and after initiation versus after touch: $t(41) = 7.94$, $p < 0.001$). Additionally, 76% of recordings showed decreased PLV at 5 Hz during initiation compared to before and after initiation (Figure 4E, paired t test, before versus during: $t(41) = 3.24$, $p = 0.002$ and after versus during: $t(41) = 3.36$, $p = 0.002$).

Average phase lags across all recordings (PFC phase minus PPC phase) were small for all three animals (Figure 4F, mean phase lags in degrees before initiation: Animal A = 27.0, Animal B = 5.4, and Animal C = −11.2 and after initiation: Animal A = 24.2, Animal B = 8.4, and Animal C = −5.92), indicating that there may be direct interactions between these regions rather than a common input to both regions. However, this is not conclusive given that the average phase lag was not consistently positive or negative across the three animals and thus it is unclear which oscillation is leading the other.

To test for directionality in the connectivity between PFC and PPC, we calculated spectral Granger causality between these brain areas. We found evidence of bi-directional effective connectivity in the theta frequency band during the sustained attention period with no clear preference for one of the two directions (Figure 4G, left: mean spectral Granger causality averaged across all animals ± 1 SEM, t test comparing directions $t(82) = 0.38$, $p = 0.70$). Interestingly, we also found evidence for effective connectivity in the beta frequency band, significantly stronger in the bottom-up direction ($t(82) = -3.45$, $p < 0.001$). During the period after touch, theta Granger causality was significantly weaker in both directions compared to the attention period (Figure 4G, right: $t(82) = -3.57$, $p < 0.001$ and $t(82) = -5.45$, $p < 0.001$). Granger causality in the beta frequency range was not different in the top-down and bottom-up directions following touch ($t(82) = -1.27$, $p = 0.21$), but was significantly weaker in the bottom-up direction after touch compared to after initiation ($t(82) = 2.28$, $p = 0.03$). Together, this provides further evidence that long-range communication during attention-demanding behavior between PFC and PPC relies on theta oscillations, and this effective connectivity is modulated according to task period.

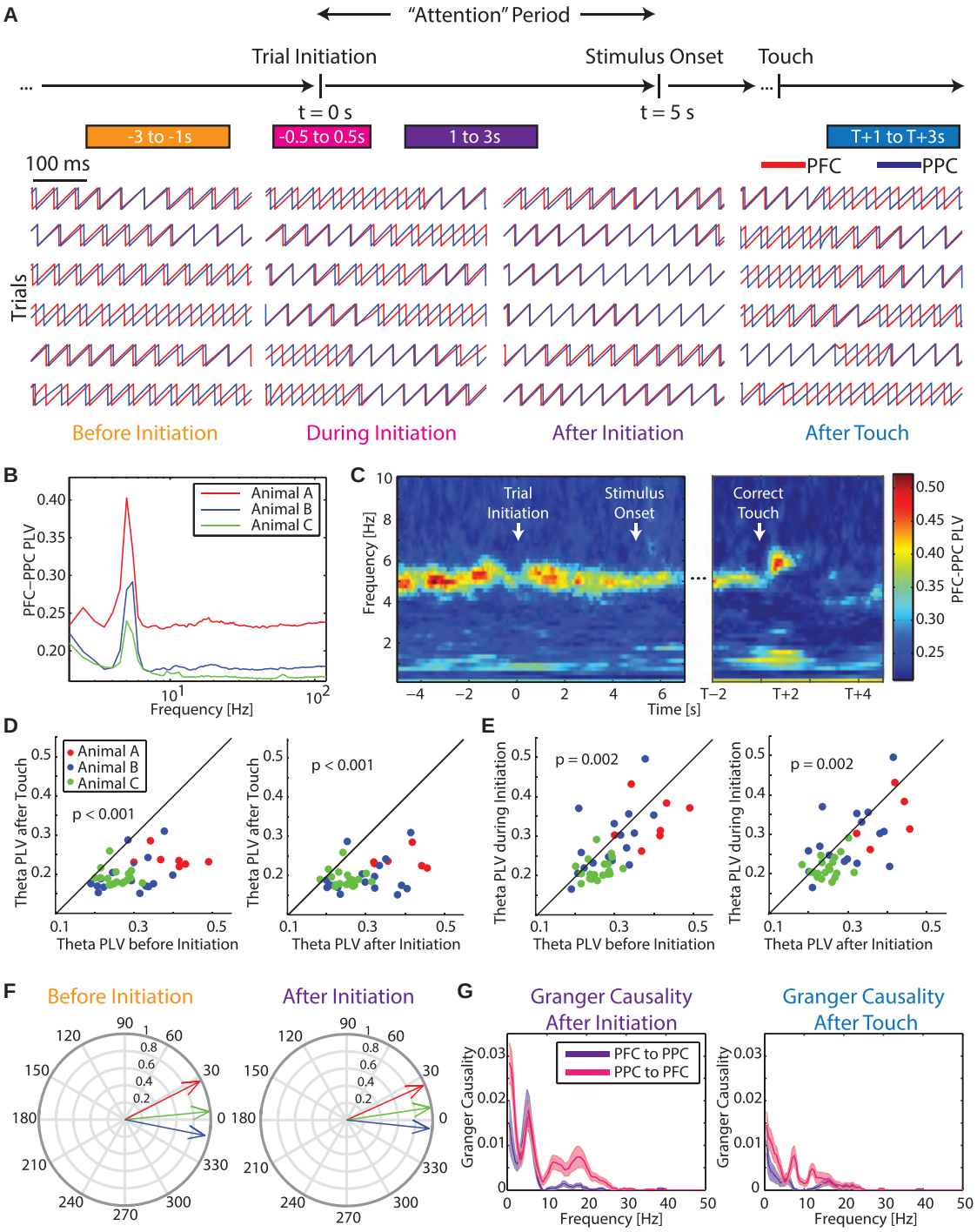

Figure 4. Effective Connectivity and Task-Dependent Synchronization between PFC and PPC at 5 Hz

(A) LFP-LFP phase locking was used to assess synchronization between PFC and PPC. At behaviorally relevant periods during the behavior task (before initiation = −3 to −1 s relative to initiation, during initiation = −0.5 to 0.5 s relative to initiation, after initiation = 1 to 3 s relative to initiation, and after touch = 1 to 3 s relative to touch) phases in PFC and PPC were assessed for consistent differences. Here, the phase at 5 Hz is shown for one pair of channels across trials.

(B) PLV was highest at 5 Hz.

(C) Averaged for Animal A, phase locking between PFC and PPC was prominent before and after trial initiation, weakened during trial initiation and by stimulus onset, and effectively abolished following touch. See Figure S4 for other animals.

(D) Phase locking values before initiation (left) and after initiation (right) were significantly greater than after touch (p values for paired t test). Each dot represents one recording session.

(legend continued on next page)

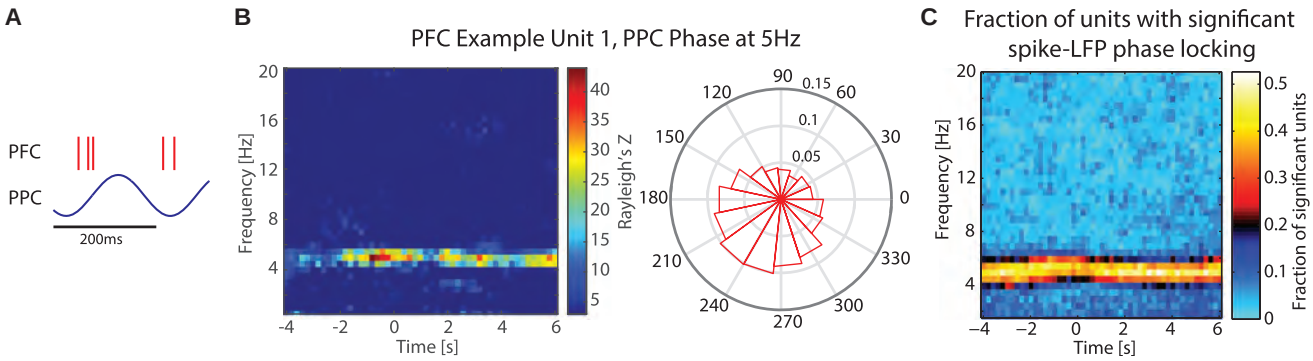

Figure 5. Spiking Activity in PFC Exhibited Long-Range Phase Locking to PPC 5 Hz Oscillation

(A) Spike-LFP phase locking was used to test if theta phase organized spiking activity across areas. The schematic shows that only a uni-directional long-range relationship was found between PPC theta phase and PFC spiking activity.

(B) An example unit recorded in PFC exhibited phase locking to PPC 5 Hz activity. The polar plot shows histogram of preferred phase of firing (in degrees).

(C) Combined across recordings for Animal A, spike-LFP phase locking was most prominent at a narrow band centered on 5 Hz, with a large fraction of units exhibiting significant spike-LFP phase locking. Spike-LFP phase locking was present throughout the duration of the trial and did not exhibit task-dependent modulation in strength. See Figure S5 for other animals.

Uni-Directional Long-Range Theta Spike-LFP Phase Locking

Theta phase synchronization and Granger causality between PFC and PPC indicate that this low-frequency oscillation may serve as the substrate for long-range cortico-cortical communication in the state of sustained attention. To confirm that this rhythmic interaction also guides spiking activity, we next assessed if spiking activity across these brain areas was also organized by theta oscillations. Specifically, we tested if the time of spiking in one area was influenced by the phase of the theta oscillation in the other area by calculating time- and frequency-resolved spike-LFP phase locking (Liebe et al., 2012; Totah et al., 2013).

SUs in PFC exhibited a lower firing rate on average compared to SUs in PPC (mean ± SD: Animal A, PFC = 13.35 ± 8.64 Hz, PPC = 16.61 ± 10.21 Hz, $t(346) = -3.17$, and $p = 0.002$; Animal B, PFC = 12.06 ± 9.45 Hz, PPC = 17.72 ± 12.99 Hz, $t(312) = -4.46$, and $p < 0.001$; and Animal C, PFC = 10.96 ± 7.30 Hz, PPC = 17.81 ± 11.38 Hz, $t(191) = -5.05$, and $p < 0.001$). Only Animal A exhibited a difference in PFC firing rate before and after trial initiation (mean PFC firing rate before and after initiation ± SD: Animal A, 12.81 ± 8.67 Hz, 13.73 ± 8.73 Hz, $t(154) = -5.12$, and $p < 0.001$), whereas Animals B and C showed different firing rates in PPC before and after trial initiation (mean PPC firing rate before and after initiation ± SD: Animal B, 16.26 ± 11.65 Hz, 18.76 ± 14.11 Hz, $t(141) = -7.45$ and $p < 0.001$ and Animal C, 16.37 ± 10.43 Hz, 18.84 ± 12.21 Hz, $t(61) = -5.95$, and $p < 0.001$). In keeping with the phase synchronization and Granger causality in the theta frequency band between PFC and PPC, we found that units in PFC were phase locked to the theta oscillation in PPC (Figure 5A, schematic). As shown by an example unit from Animal A, spike-LFP phase locking was centered on a narrow band at 5 Hz (Figure 5B), and the distribution of phases of each spike is shown in a polar histogram (see Figure S5C for the distribution of preferred phases for all PFC units with significant spike-LFP phase locking to the 5 Hz oscillation in PPC). Of the 449 PFC unit, PPC phase pairs analyzed (Animal A = 152, Animal B = 168, and Animal C = 129), 30.5% exhibited theta spike-LFP locking (Animal A = 60.5%, Animal B = 13.7%, and Animal C = 17.1%), as defined by significant theta spike-LFP phase locking for at least 20% of the trial (Figure 5C, fraction of significantly phase-locking units across time for Animal A, see Figures S5A and S5B for other animals). Interestingly, phase locking of PFC units to PPC phase did not exhibit any significant fluctuations in strength across the duration of the trial (ANOVA: $F(2,728) = 0.41$, $p = 0.66$). Furthermore, across all recordings, there was no significant change in the fraction of units which exhibited spike-LFP phase locking (ANOVA, $F(2,114) = 1.67$, $p = 0.19$). There was weak correlation between firing rate and strength of spike-LFP phase locking, significant for two animals (correlation coefficients: Animal A = 0.17, $p = 0.03$; Animal B = 0.09, $p = 0.22$; and Animal C = 0.31, $p < 0.001$).

In contrast, there was no sizeable phase locking of PPC units to theta oscillations in PFC. Of the 393 PPC unit, PFC phase pairs analyzed (Animal A = 189, Animal B = 142, and Animal C = 62), only 1.8% exhibited theta spike-LFP locking (Figures S5D–S5F; Animal A = 1.6%, Animal B = 2.1%, and Animal C = 1.6%). There

(E) Phase locking values before initiation (left) and after initiation (right) were significantly greater than during initiation (p values for paired t test).

(F) The phase difference between PFC and PPC was near zero for all animals, both before initiation and after initiation. The plot shows the proportion of recordings versus phase differences in degrees.

(G) Pairwise spectral Granger causality was calculated on the median LFP in each brain area during the sustained attention period (left) and after touch (right). Bi-directional effective connectivity in the theta range and bottom-up effective connectivity in the beta frequency range were evident during the attention period. Both of these forms of communication are decreased in the period after touch. The lines represent mean across recordings, shaded areas represent ± 1 SEM.

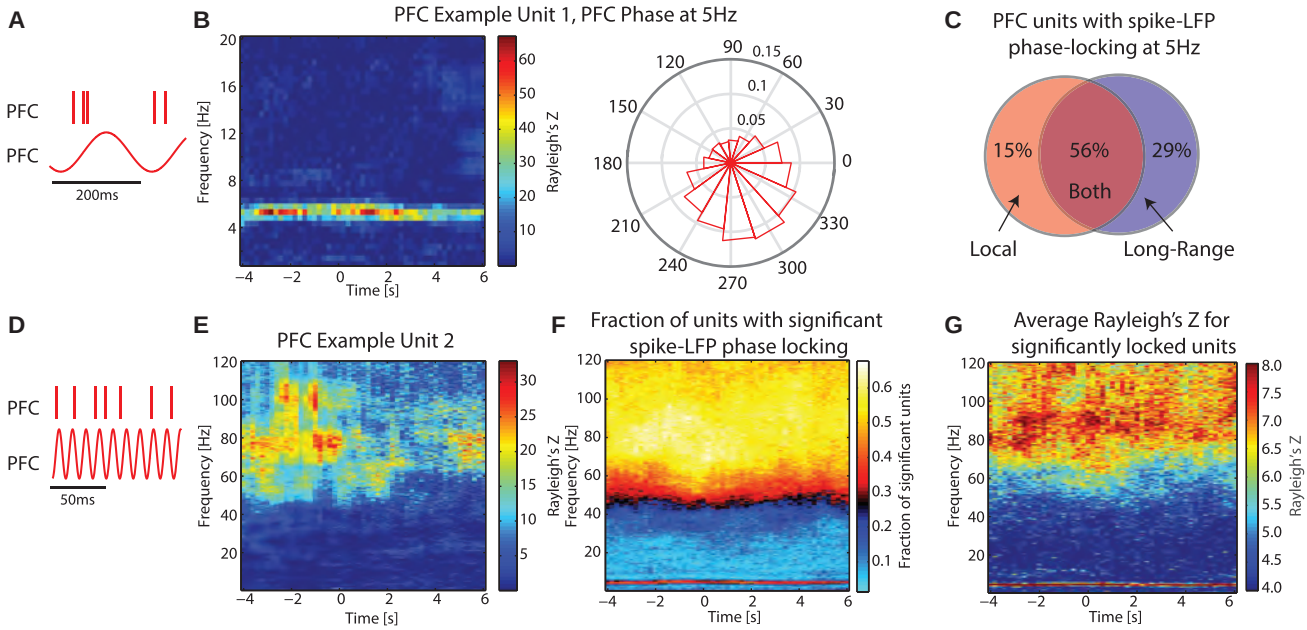

Figure 6. Both Theta and High Gamma Activity Were Involved in the Local Organization of Spiking Activity in PFC

(A) Spike-LFP phase locking was calculated between the 5 Hz oscillation and spiking activity, both in PFC.

(B) An example unit recorded in PFC exhibited phase locking to PFC 5 Hz activity. The polar plot shows preferred phase of firing, same unit as Figure 5B.

(C) PFC units exhibited local and long-range spike-LFP phase locking to the 5 Hz oscillation. The Venn diagram indicates the percentage of units across all animals that exhibited local locking to PFC phase, long-range locking to PPC phase, or both local and long-range locking.

(D) Spike-LFP phase locking was calculated between high-gamma activity and spiking activity, both in PFC.

(E) An example unit recorded in PFC exhibited phase locking to broad high-gamma activity.

(F) Across recordings for Animal A, units were predominantly phase locked to oscillations at 5 Hz and activity in the high gamma band.

(G) Across recordings for Animal A, the average Rayleigh's Z for significantly locked units (a measure of the strength of phase locking) was also highest for spike-LFP phase locking at 5 Hz and in the high gamma range.

was weak negative correlation between firing rate and strength of spike-LFP phase locking (correlation coefficients: Animal A = −0.22, p = 0.003; Animal B = −0.21, p = 0.01; and Animal C = −0.35, p = 0.005). This uni-directional coupling of PFC spikes to the PPC theta phase is in contrast to our finding of bi-directional effectivity connectivity measured with Granger causality. This discrepancy may shed light on the differences in information contained in suprathreshold (spiking) versus subthreshold (spectral power) signals.

Local Theta and High Gamma Spike-LFP Phase Locking in PFC

Having established the importance of theta oscillations for the long-range coupling of PFC and PPC, we next sought to investigate whether theta oscillations were also implicated in the organization of local processing within each brain area. In principle, both long-range and local processing could rely on the theta oscillation. However, an alternative possibility is that local and long-range synchronization are mediated by different frequencies. In order to disambiguate between these possibilities, we investigated within-area spike-LFP phase locking (phase and units from the same brain area, on neighboring electrodes) across a broad range of frequencies.

We found that both theta and broad high gamma (80–120 Hz) are relevant for local organization of spiking activity. An example unit exhibited strong spike-LFP phase locking at 5 Hz (Figures 6A and 6B). Calculating spike-LFP phase locking with the despiked LFP showed similar locking at 5 Hz (Figure S6A). See Figure S7C for the distribution of preferred phase of firing for all PFC units with significant spike-LFP phase locking to the 5 Hz oscillation in PFC. Having established that theta oscillations contribute to both local and long-range organization of PFC spiking activity, we wanted to see whether given units exhibited one or both organization schemes. Of all PFC units with significant spike-LFP phase locking, 56% (n = 90) exhibited significant spike-LFP phase locking to both local theta oscillations in PFC and long-range oscillations in PPC, while 15% (n = 24) and 29% (n = 47) exhibited only local or long-range locking, respectively (Figure 6C).

Another example PFC unit illustrates spike-LFP phase locking broadly in the high gamma frequencies (Figures 6D and 6E). Again, the spike-LFP synchrony was not an artifact of bleed through spiking activity, as the same profile is evident when using despiked LFP for the calculation (Figure S6B).

At the group level, 447 PFC unit, PFC phase pairs were analyzed (Animal A = 152, Animal B = 168, and Animal C = 127). 25.5% percent exhibited theta spike-LFP locking (Animal A = 50.7%, Animal B = 10.1%, and Animal C = 15.8%) and 57.5% to 72.9% exhibited high gamma spike-LFP locking in the 80–120 Hz range (Animal A = 66.5% to 82.9%, Animal

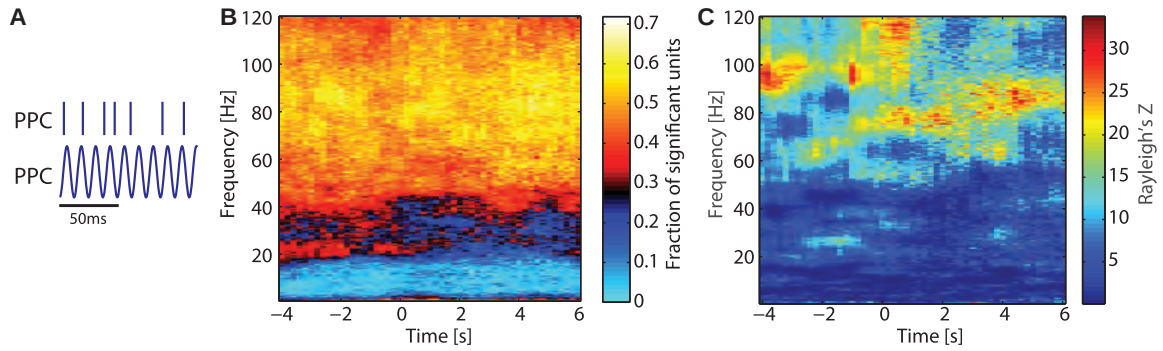

Figure 7. Spiking Activity in PPC Was Coupled to High Gamma Activity

(A) Spike-LFP phase locking was calculated between high-gamma activity and spiking activity, both in PPC.

(B) Across recordings in Animal C, units were predominantly phase locked to high-gamma activity. In contrast to PFC, no prominent spike-LFP phase locking was seen at 5 Hz.

(C) An example unit recorded in PPC exhibited phase locking to broad high-gamma activity.

B = 48.8% to 60.7%, and Animal C = 58.3% to 77.2%) (Figure 6F, Animal A; see Figures S7A and S7B for other animals). In addition to a greater fraction of units being significantly phase locked to theta and high gamma, the strength of spike-LFP phase locking was greater in these frequencies compared to alpha, beta, and gamma frequencies (Figure 6G, average strength of significant spike-LFP phase locking for Animal A). Spike-LFP phase locking to the theta oscillation was only weakly correlated to overall firing rates in one animal (Animal A, correlation coefficient = 0.18, p = 0.03).

High Gamma Spike-LFP Phase Locking Locally in PPC

We next asked if phase locking to the theta oscillation and high gamma activity is a general principle that is shared by PFC and PPC. To answer this question, we performed the same analysis as above, but for PPC units. PPC units showed strong spike-LFP phase locking to high gamma phase, a much smaller subset of PFC units exhibited spike-LFP phase locking to the theta phase. Of the PPC unit, PPC phase pairs analyzed (Animal A = 189, Animal B = 142, and Animal C = 64), 8.4% percent exhibited theta spike-LFP locking (Figure 7B, Animal C; see Figures S7D and S7E for other animals; Animal A = 9.0%, Animal B = 9.2%, and Animal C = 4.7%), while 58.0% to 70.0% exhibited high gamma spike-LFP locking in the 80–120 Hz range (Animal A = 70.4% to 79.4%, Animal B = 43.7% to 55.6%, and Animal C = 53.1% to 73.4%). Similar to the example unit in PFC, spike-LFP phase locking across broad high gamma frequencies is apparent in an example PPC unit (Figure 7C). The relative fraction of units in PPC with local theta coupling differs from the local organization of PFC units.

Taken together, this work points to the coordination of low-frequency (theta) and high-frequency (high gamma, 80–120 Hz) activity in organizing spiking activity.

DISCUSSION

We found that PFC and PPC exhibited effective connectivity and task-dependent synchronization in the theta frequency band selectively during a sustained attention task in a freely moving animal. PFC spiking was phase locked to local theta oscillations, local high-gamma activity, and to long-range PPC theta oscillations. PPC spiking was primarily phase locked to local high-gamma activity. This suggests that overall regulation of neuronal processing during sustained attention is coordinated by a combination of local and long-range activity, relying on different frequencies.

Relevance of PFC and PPC to Sustained Attention

Attention is a broad construct that has been defined as "the selective prioritization of the neural representations that are most relevant to one's current behavioral goal" (Buschman and Kastner, 2015). Sustained attention, one facet of overall attention, involves focusing on one task for a continuous amount of time. The behavioral task in this study, the 5-CSRTT, includes aspects of the continuous performance task used in humans and has been used extensively in assessing sustained attention in animals (Robbins, 1998). We recorded from PFC in the rostral-most portion of the anterior sigmoid gyrus, similar to previous studies (Fritz et al., 2010) and the caudal portion of PPC located on the suprasylvian gyrus. This area of PFC in ferrets has been shown to have reciprocal connections with the mediodorsal nucleus of the thalamus (Duque and McCormick, 2010) and appears to be responsible for behaviorally relevant selection of sensory stimuli (Fritz et al., 2010; Zhou et al., 2016). Our recording and tracer injection locations agreed with localization of PPC as previously defined in the ferret (Manger et al., 2002; Foxworthy and Meredith, 2011; Foxworthy et al., 2013).

Through anterograde and retrograde tracing, we found that these areas in the ferret exhibit direct anatomical connections. In humans, direct frontoparietal connectivity assessed using diffusion tensor imaging found that the strength of white-matter fibers is related to the efficiency of attentional selection in visuospatial tasks (Tuch et al., 2005). Taken together, our tracing results suggest that in ferrets, these regions of PFC and PPC may be homologous to aspects of the frontoparietal attention network in the non-human primate and human brains.

Extensive work in animals and humans has demonstrated the importance of the frontoparietal network, and in particular PFC

and PPC, in mediating attention and cognitive control (Katsuki and Constantinidis, 2012). Inactivation of PFC in monkeys with muscimol injection resulted in a deficit in selective attention performance (Iba and Sawaguchi, 2003) and muscimol inactivation in both FEF (Wardak et al., 2006) and PPC (Wardak et al., 2004) resulted in deficits in visual attention. Lesion and imaging studies in humans have revealed that activation of frontal and parietal cortical areas is associated with performance on sustained attention tasks (Sarter et al., 2001; Kastner and Ungerleider, 2000). Our findings contribute to this body of work by elucidating similarities and differences in how activity in these brain areas is organized during sustained attention. The organization of activity across these areas not only provides further support for the importance of coordinated activity in these brain regions for mediating attentional processing, but also provides further insight into the mechanism of such communication. For further discussion see the Discussion section, Conceptual Model and Conclusions.

Importance of Theta and High Gamma Oscillations in Cognition

A framework for the role of cortical oscillations in sustained attention has recently been proposed: frontomedial theta oscillations mediate cognitive monitoring and control functions, low-frequency phase synchronization mediates communication across brain networks, gamma activity mediates excitation of task-relevant cortical areas, and alpha oscillations mediate inhibition of task-irrelevant cortical areas (Clayton et al., 2015). Our results provide further evidence for these organizing principles. We found task-modulated phase locking in the theta band between PFC and PPC and evidence of bi-directional effective connectivity. Importantly, PLV between PFC and PPC was abolished following the behavioral touch response. Thus, phase locking between PFC and PPC appears to be behaviorally relevant as this communication mode is isolated to periods of the task leading up to and during sustained attention. Our Granger causality result further supports this finding.

It should be noted that substantial work conducted in the frontoparietal network has found beta synchronization to play an important role in long-range synchronization mediating attention (Womelsdorf and Everling, 2015; Hipp et al., 2011; Gross et al., 2004). In this study, we found bottom-up effective connectivity from PPC to PFC in the beta frequency range using Granger causality, but not top-down connectivity. Effective connectivity was significantly weaker following correct touch. Continued work will be needed to clarify modes of long-range synchronization as a function of specific brain networks and behavioral demands.

Organization of Spiking Activity by Oscillations

The organization of spiking activity and oscillations is critical for the effective integration of relevant task information. Compared to phase locking between PFC and PPC, it remains less apparent to what extent spike-LFP phase locking was functionally relevant in the attention task. We found that PFC units were phase locked to the theta oscillation in both PFC and PPC, whereas PPC units were less prominently phase locked to theta in PFC or PPC. This suggests that theta oscillations in PFC and PPC have differential roles in organizing spiking activity. Indeed, we found a local peak in PPC spectral activity in the theta band that increased during the sustained attention period, while PFC showed no such spectral peak or modulation. The lack of a theta peak in PFC could theoretically result from difficulty detecting spike-LFP phase locking because of the low-amplitude signal. However, we exclude this alternate explanation because strong local coupling was found between PFC spikes and PFC theta phase. It remains an outstanding question why fewer PPC units were phase locked to the local theta oscillation. While small, this subset of units may be serving an important function role. The activity of PPC units could be reflecting environmental sampling, while the theta oscillation in PPC acts as a more global pacemaker, synchronizing with PFC to establish the PFC theta oscillation and guide spiking activity in PFC.

The emergence of theta as a fundamental rhythm for the coordination of activity across cortical areas may depend on the behavioral paradigm used. Most previous investigations of the electrophysiology of sustained attention required animals to be head fixed. Visual stimuli were presented, and animals indicated trained responses by making or inhibiting saccades. These experiments provided excellent early insight into neural correlates underlying sustained attention. However, these experiments included fundamental shortcomings by restricting movement-related exploration. Head fixation precludes natural movement and places the animal in an artificial state of limited behavior. In the present study, we implemented a sustained attention task in which the animals were freely moving. Even in the context of a trained task, free movement allows for a broader range of behavioral actions and likely, underlying network dynamics. Therefore, the reported mechanisms of attentional processing likely more closely reflect neuronal processing during sustained attention in untrained everyday behavior. In particular, theta oscillations, which have previously been implicated in hippocampus for coordinating exploration and navigation, may have additional roles in neocortex for mediating attention in ethological tasks.

Conceptual Model and Conclusions

Taken together, our findings demonstrate that the simultaneous organization of spiking activity by multiple frequencies mediates local and long-range connectivity during cognitively demanding behavior. Theta oscillations mediated the long-range synchronization of PFC and PPC in a task-dependent manner. PFC exhibited local coupling of spiking activity to both theta and high gamma activity, while PPC spiking was primarily locally phase locked to high gamma activity. PPC was more sensitive to task-modulation of spectral power than PFC. Given that PPC receives input from a number of sensory areas, it is not surprising that this region is more sensitive to salient sensory input compared to higher-order PFC. Interestingly, the phase synchronization of PFC and PPC was also transiently disrupted during the sensory signals. In general, theta activity in cortex may reflect connectivity in absence of sensory input (e.g., a default mode network). During such states, PFC and PPC may synchronize in order to communicate about expectation, top-down allocation of resources, etc. The onset of sensory stimuli may induce a network state change in which PPC momentarily decouples from PFC and allocates

resources to the processing of relevant sensory cues. In support of such a model, PPC exhibited concentrations of SU structural break points, or significant modulation of firing rate, at these two behaviorally relevant time points. Taken one step further, this may also explain why fewer PPC units exhibited phase locking to the theta oscillation. PPC spiking activity may encode information about incoming sensory cues, rather than top-down expectation or program execution from PFC. In contrast, spiking in PFC was sensitive to bottom-up input from PPC, communicated through the phase of theta oscillations.

EXPERIMENTAL PROCEDURES

Behavioral Task

See the Supplemental Information for more details about procedures. All animal procedures were approved by the Institutional Animal Care and Use Committee of the University of North Carolina at Chapel Hill and complied with guidelines set by the NIH. Experiments were conducted using spayed female ferrets (*Mustela putorius furo*, n = 3 for behavior and electrophysiology, n = 4 for anatomical studies). A custom-built behavioral box was used for touch-screen implementation of the 5-CSRTT (Bari et al., 2008) (Figure 1B).

Animals were trained and tested once daily on a 5 days on/2 days off schedule. Animals were water restricted to enhance participation in the behavioral task. Animals initiated trials at the lick spout to trigger a 5 s delay period ("sustained attention"). Following this, one of the five windows displayed a white square filling the response area for 3.5 s. A correct response was defined as touching this window during this 3.5 s stimulation period or the 2 s following.

Microelectrode Array Implantation Surgery

Animals were implanted with microelectrode arrays in both PFC and PPC. Aseptic surgical procedures were used, as previously described (Sellers et al., 2013, 2015); also see the Supplemental Information. Two small craniotomies were made to access the right hemisphere of PFC and PPC. 32-channel microelectrode arrays (tungsten electrodes oriented 4 × 8, 200 μm spacing, low impedance reference electrode 1 mm shorter on the same array) were inserted into deep layers of cortex and secured using dental cement.

In Vivo Electrophysiological Recordings

Continuous electrophysiological data were acquired at a sampling rate of 20 kHz. A motorized commutator was used to allow unencumbered animal movement during electrophysiology. Behavioral responses were recorded as digital inputs together with the electrophysiology to ensure proper synchronization of neuronal activity and behavior.

Data Analysis

Trial initiation was used for alignment of trials (−5 to 7 s relative to trial initiation). The 5 s following initiation represent the sustained attention period. For a subset of analyses, we additionally looked at neuronal activity aligned to screen touch, ranging from −2 to 5 s relative to touch. We only analyzed trials with correct responses, in which the animal was facing the screen at the time of stimulus onset.

Spectral analysis was performed by convolving the LFP signals with a family of Morlet wavelets. Standard definitions of frequency bands were used for initial exploratory analysis (delta = 0.5–4 Hz, theta = 4–8 Hz, alpha = 8–12 Hz, beta = 12–30 Hz, gamma = 30–80 Hz, and high gamma = 80–120 Hz). We found that the LFP spectra of all animals exhibited a pronounced peak at 5 Hz and thus used this frequency for subsequent theta analysis. We also found that each animal exhibited a local peak in or close to the gamma frequency range (29 Hz, 34 Hz, and 33 Hz, respectively) in PPC during the sustained attention period, we thus centered a 10 Hz-wide band around this local peak for each animal for analysis of gamma power in PPC.

Spikes were sorted into putative SUs using standard methods (Offline Sorter, Plexon). A structural change test (Chow, 1960; Kimchi and Laubach, 2009) was used to assess if the SU firing rate was significantly modulated over the course of the peristimulus time period. PLV between LFP signals in the two brain regions were calculated as previously described (Lachaux et al., 1999; Liebe et al., 2012). Pairwise spectral Granger causality was calculated using the GCCA Toolbox (Seth, 2010) to test for effective connectivity between PFC and PPC from 0.5 to 50 Hz. In order to assess the degree of phase locking of SUs as a function of time and frequency, we calculated spike-LFP synchrony according to methods previously described (Totah et al., 2013).

Tracing Studies

Two types of tracer studies were completed to establish the presence of direct anatomical projections from PFC to PPC. Anterograde virus, rAAV5-CamKII-GFP, was injected in PFC or retrograde tracer Alexa 488-conjugated CTB was injected in PPC (Conte et al., 2009).

SUPPLEMENTAL INFORMATION

Supplemental Information includes Supplemental Experimental Procedures and seven figures and can be found with this article online at http://dx.doi.org/10.1016/j.celrep.2016.08.055.

AUTHOR CONTRIBUTIONS

K.K.S., C.Y., Z.C.Z., and F.F. designed the experiments. K.K.S. performed the experiments. K.K.S., I.S., S.A., and F.F. analyzed the data. Y.L. and I.S. validated the data analysis. S.R.-S. provided brain atlas and cross-checked anatomy data. K.K.S. and F.F. wrote the paper.

ACKNOWLEDGMENTS

The authors would like to thank present and past members of the F.F lab for their support, in particular, Carrington Merritt, Matthew Wilson, and Stephen Schmidt. The authors would like to acknowledge Jennifer Bizley and Stephen Town for aid with the apparatus and task design. This work was in part funded by UNC Department of Psychiatry, a donation by Dean and Brenda Proctor, the Human Frontier Science Program, and by the National Institute of Mental Health of the NIH under award no. R01MH101547. The content is solely the responsibility of the authors and does not necessarily represent the official views of the NIH. Imaging was supported by the UNC Confocal and Multiphoton Imaging Core of NINDS Center Grant P30 NS045892.

Received: May 17, 2016
Revised: July 15, 2016
Accepted: August 17, 2016
Published: September 13, 2016

REFERENCES

Bari, A., Dalley, J.W., and Robbins, T.W. (2008). The application of the 5-choice serial reaction time task for the assessment of visual attentional processes and impulse control in rats. Nat. Protoc. *3*, 759–767.

Buschman, T.J., and Miller, E.K. (2007). Top-down versus bottom-up control of attention in the prefrontal and posterior parietal cortices. Science *315*, 1860–1862.

Buschman, T.J., and Kastner, S. (2015). From behavior to neural dynamics: an integrated theory of attention. Neuron *88*, 127–144.

Buzsáki, G., and Draguhn, A. (2004). Neuronal oscillations in cortical networks. Science *304*, 1926–1929.

Canolty, R.T., Ganguly, K., Kennerley, S.W., Cadieu, C.F., Koepsell, K., Wallis, J.D., and Carmena, J.M. (2010). Oscillatory phase coupling coordinates anatomically dispersed functional cell assemblies. Proc. Natl. Acad. Sci. USA *107*, 17356–17361.

Carli, M., Robbins, T.W., Evenden, J.L., and Everitt, B.J. (1983). Effects of lesions to ascending noradrenergic neurones on performance of a 5-choice serial reaction task in rats; implications for theories of dorsal noradrenergic bundle function based on selective attention and arousal. Behav. Brain Res. *9*, 361–380.

Cavada, C., and Goldman-Rakic, P.S. (1989). Posterior parietal cortex in rhesus monkey: II. Evidence for segregated corticocortical networks linking sensory and limbic areas with the frontal lobe. J. Comp. Neurol. *287*, 422–445.

Chow, G. (1960). Tests of equality between sets of coefficients in two linear regressions. Econometrica *28*, 591–605.

Clayton, M.S., Yeung, N., and Cohen Kadosh, R. (2015). The roles of cortical oscillations in sustained attention. Trends Cogn. Sci. *19*, 188–195.

Conte, W.L., Kamishina, H., and Reep, R.L. (2009). Multiple neuroanatomical tract-tracing using fluorescent Alexa Fluor conjugates of cholera toxin subunit B in rats. Nat. Protoc. *4*, 1157–1166.

Corbetta, M., and Shulman, G.L. (2002). Control of goal-directed and stimulus-driven attention in the brain. Nat. Rev. Neurosci. *3*, 201–215.

Duque, A., and McCormick, D.A. (2010). Circuit-based localization of ferret prefrontal cortex. Cereb. Cortex *20*, 1020–1036.

Engel, A.K., Fries, P., and Singer, W. (2001). Dynamic predictions: oscillations and synchrony in top-down processing. Nat. Rev. Neurosci. *2*, 704–716.

Foxworthy, W.A., and Meredith, M.A. (2011). An examination of somatosensory area SIII in ferret cortex. Somatosens. Mot. Res. *28*, 1–10.

Foxworthy, W.A., Allman, B.L., Keniston, L.P., and Meredith, M.A. (2013). Multisensory and unisensory neurons in ferret parietal cortex exhibit distinct functional properties. Eur. J. Neurosci. *37*, 910–923.

Fries, P. (2005). A mechanism for cognitive dynamics: neuronal communication through neuronal coherence. Trends Cogn. Sci. *9*, 474–480.

Fries, P. (2009). Neuronal gamma-band synchronization as a fundamental process in cortical computation. Annu. Rev. Neurosci. *32*, 209–224.

Fritz, J.B., David, S.V., Radtke-Schuller, S., Yin, P., and Shamma, S.A. (2010). Adaptive, behaviorally gated, persistent encoding of task-relevant auditory information in ferret frontal cortex. Nat. Neurosci. *13*, 1011–1019.

Gross, J., Schmitz, F., Schnitzler, I., Kessler, K., Shapiro, K., Hommel, B., and Schnitzler, A. (2004). Modulation of long-range neural synchrony reflects temporal limitations of visual attention in humans. Proc. Natl. Acad. Sci. USA *101*, 13050–13055.

Hipp, J.F., Engel, A.K., and Siegel, M. (2011). Oscillatory synchronization in large-scale cortical networks predicts perception. Neuron *69*, 387–396.

Iba, M., and Sawaguchi, T. (2003). Involvement of the dorsolateral prefrontal cortex of monkeys in visuospatial target selection. J. Neurophysiol. *89*, 587–599.

Kastner, S., and Ungerleider, L.G. (2000). Mechanisms of visual attention in the human cortex. Annu. Rev. Neurosci. *23*, 315–341.

Katsuki, F., and Constantinidis, C. (2012). Unique and shared roles of the posterior parietal and dorsolateral prefrontal cortex in cognitive functions. Front. Integr. Nuerosci. *6*, 17.

Kimchi, E.Y., and Laubach, M. (2009). Dynamic encoding of action selection by the medial striatum. J. Neurosci. *29*, 3148–3159.

Kopell, N., Ermentrout, G.B., Whittington, M.A., and Traub, R.D. (2000). Gamma rhythms and beta rhythms have different synchronization properties. Proc. Natl. Acad. Sci. USA *97*, 1867–1872.

Lachaux, J.P., Rodriguez, E., Martinerie, J., and Varela, F.J. (1999). Measuring phase synchrony in brain signals. Hum. Brain Mapp. *8*, 194–208.

Langner, R., and Eickhoff, S.B. (2013). Sustaining attention to simple tasks: a meta-analytic review of the neural mechanisms of vigilant attention. Psychol. Bull. *139*, 870–900.

Liebe, S., Hoerzer, G.M., Logothetis, N.K., and Rainer, G. (2012). Theta coupling between V4 and prefrontal cortex predicts visual short-term memory performance. Nat. Neurosci. *15*, 456–462, S1–S2.

Lisman, J.E., and Jensen, O. (2013). The θ-γ neural code. Neuron *77*, 1002–1016.

Manger, P.R., Masiello, I., and Innocenti, G.M. (2002). Areal organization of the posterior parietal cortex of the ferret (Mustela putorius). Cereb. Cortex *12*, 1280–1297.

Petersen, S.E., and Posner, M.I. (2012). The attention system of the human brain: 20 years after. Annu. Rev. Neurosci. *35*, 73–89.

Posner, M.I., and Petersen, S.E. (1990). The attention system of the human brain. Annu. Rev. Neurosci. *13*, 25–42.

Robbins, T.W. (1998). Arousal and attention: psychopharmacological and neuropsychological studies in experimental animals. In The Attentive Brain, R. Parasuraman, ed. (Cambridge: MIT Press).

Sarnthein, J., Petsche, H., Rappelsberger, P., Shaw, G.L., and von Stein, A. (1998). Synchronization between prefrontal and posterior association cortex during human working memory. Proc. Natl. Acad. Sci. USA *95*, 7092–7096.

Sarter, M., Givens, B., and Bruno, J.P. (2001). The cognitive neuroscience of sustained attention: where top-down meets bottom-up. Brain Res. Brain Res. Rev. *35*, 146–160.

Scolari, M., Seidl-Rathkopf, K.N., and Kastner, S. (2015). Functions of the human frontoparietal attention network: Evidence from neuroimaging. Curr Opin Behav Sci *1*, 32–39.

Sellers, K.K., Bennett, D.V., Hutt, A., and Fröhlich, F. (2013). Anesthesia differentially modulates spontaneous network dynamics by cortical area and layer. J. Neurophysiol. *110*, 2739–2751.

Sellers, K.K., Bennett, D.V., Hutt, A., Williams, J.H., and Fröhlich, F. (2015). Awake vs. anesthetized: layer-specific sensory processing in visual cortex and functional connectivity between cortical areas. J. Neurophysiol. *113*, 3798–3815.

Seth, A.K. (2010). A MATLAB toolbox for Granger causal connectivity analysis. J. Neurosci. Methods *186*, 262–273.

Siegel, M., Warden, M.R., and Miller, E.K. (2009). Phase-dependent neuronal coding of objects in short-term memory. Proc. Natl. Acad. Sci. USA *106*, 21341–21346.

Szczepanski, S.M., Pinsk, M.A., Douglas, M.M., Kastner, S., and Saalmann, Y.B. (2013). Functional and structural architecture of the human dorsal frontoparietal attention network. Proc. Natl. Acad. Sci. USA *110*, 15806–15811.

Totah, N.K., Jackson, M.E., and Moghaddam, B. (2013). Preparatory attention relies on dynamic interactions between prelimbic cortex and anterior cingulate cortex. Cereb. Cortex *23*, 729–738.

Tuch, D.S., Salat, D.H., Wisco, J.J., Zaleta, A.K., Hevelone, N.D., and Rosas, H.D. (2005). Choice reaction time performance correlates with diffusion anisotropy in white matter pathways supporting visuospatial attention. Proc. Natl. Acad. Sci. USA *102*, 12212–12217.

Varela, F., Lachaux, J.P., Rodriguez, E., and Martinerie, J. (2001). The brainweb: phase synchronization and large-scale integration. Nat. Rev. Neurosci. *2*, 229–239.

von Stein, A., Chiang, C., and König, P. (2000). Top-down processing mediated by interareal synchronization. Proc. Natl. Acad. Sci. USA *97*, 14748–14753.

Voytek, B., and Knight, R.T. (2015). Dynamic network communication as a unifying neural basis for cognition, development, aging, and disease. Biol. Psychiatry *77*, 1089–1097.

Wardak, C., Olivier, E., and Duhamel, J.R. (2004). A deficit in covert attention after parietal cortex inactivation in the monkey. Neuron *42*, 501–508.

Wardak, C., Ibos, G., Duhamel, J.R., and Olivier, E. (2006). Contribution of the monkey frontal eye field to covert visual attention. J. Neurosci. *26*, 4228–4235.

Womelsdorf, T., and Fries, P. (2007). The role of neuronal synchronization in selective attention. Curr. Opin. Neurobiol. *17*, 154–160.

Womelsdorf, T., and Everling, S. (2015). Long-range attention networks: circuit motifs underlying endogenously controlled stimulus selection. Trends Neurosci. *38*, 682–700.

Zhou, Z.C., Yu, C., Sellers, K.K., and Fröhlich, F. (2016). Dorso-lateral frontal cortex of the ferret encodes perceptual difficulty during visual discrimination. Sci. Rep. *6*, 23568.